The Formation and Coarsening of the Concertina Pattern

Jutta Steiner

PIRE and OxMOS Workshop Oxford

Joint work with
F. Otto (MPI Leipzig)
R. Schäfer, H. Wieczoreck (IFW Dresden)

Experiment: Magnetization reversal

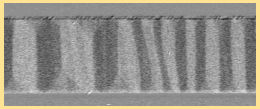

. . . in thin elongated ferromagnetic elements

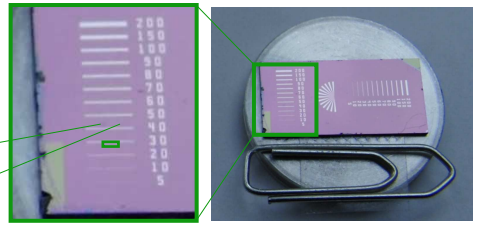

Permalloy, width $\ell = 30\mu\text{m}$, thickness $t = 60\text{nm}$

magnetic field H_{ext}

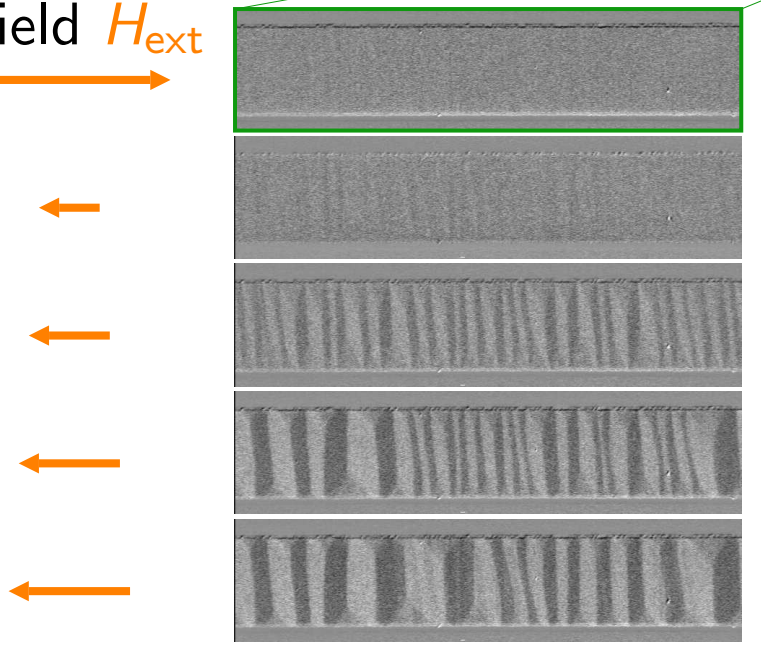

Experiment: Magnetization reversal

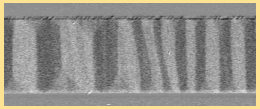

. . . in thin elongated ferromagnetic elements

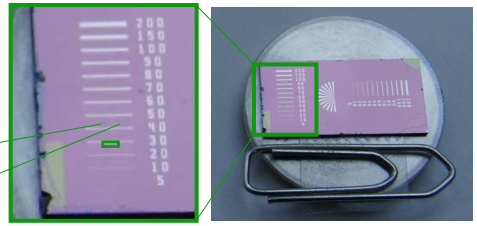

Permalloy, width $\ell = 30\mu\text{m}$, thickness $t = 60\text{nm}$

magnetic field H_{ext}

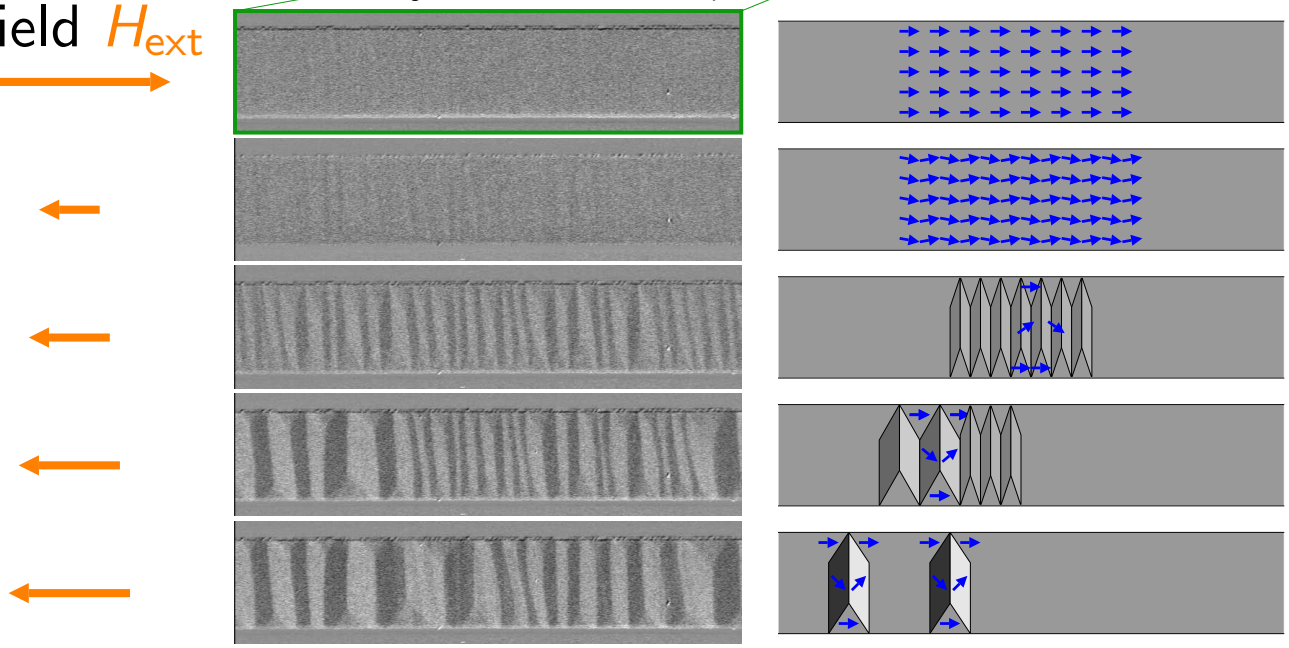

Experiment: Magnetization reversal

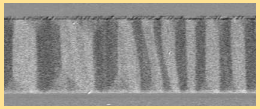

. . . in thin elongated ferromagnetic elements

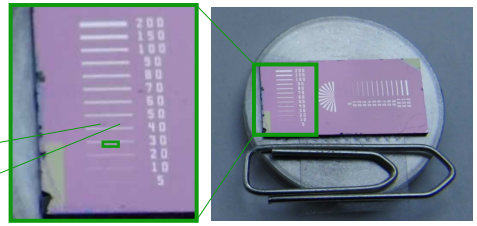

Permalloy, width $\ell = 30\mu\text{m}$, thickness $t = 60\text{nm}$

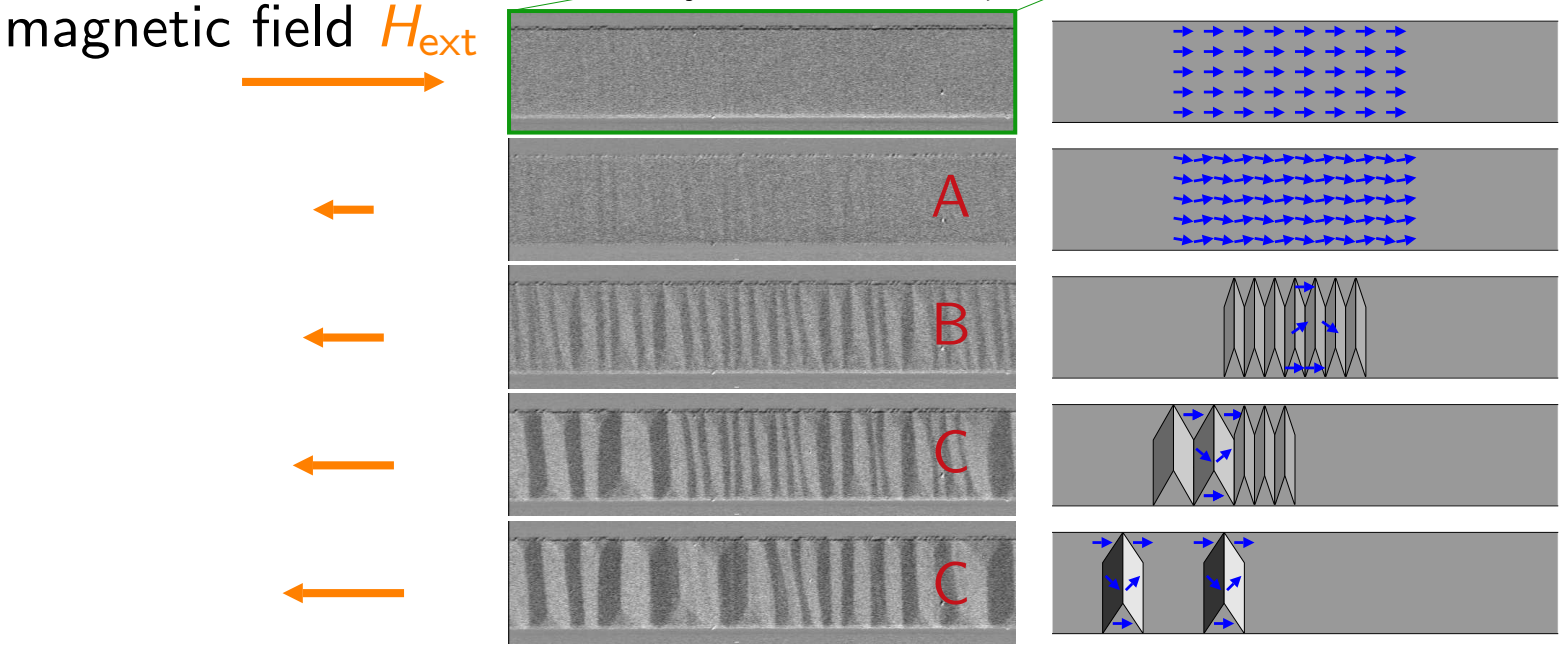

Goal: Use asymptotic analysis and numerical simulation to understand

- A Instability at critical field $H_{\text{ext}} = H^*_{\text{ext}}$
- B Formation of domain pattern
- C Coarsening

Variational continuum model by Landau & Lifschitz (1/2)

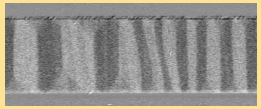

- Periodic sample
  $\Omega = \mathbb{R} \times (0, \ell) \times (0, t)$
  width ℓ, thickness t

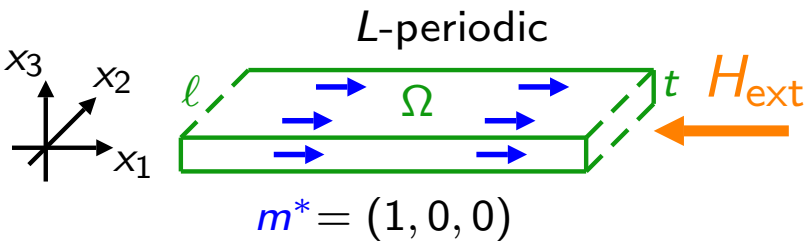

- External magnetic field $H_{\text{ext}} = (-h_{\text{ext}}, 0, 0)$
- Magnetization $m = (m_1, m_2, m_3)$, $|m|^2 = 1$

Variational continuum model by Landau & Lifschitz (1/2)

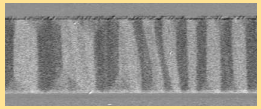

- Periodic sample
  $\Omega = \mathbb{R} \times (0, \ell) \times (0, t)$
  width ℓ, thickness t

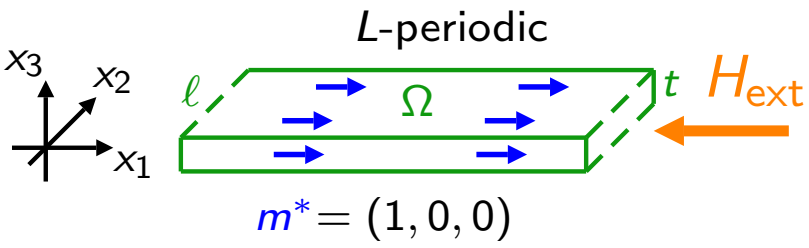

- External magnetic field $H_{\text{ext}} = (-h_{\text{ext}}, 0, 0)$
- Magnetization $m = (m_1, m_2, m_3)$, $|m|^2 = 1$

Observed configuration $\Leftrightarrow$ Minimizer of the micromagnetic energy

$$E(m) = \underbrace{d^2 \int_\Omega |\nabla m|^2 \, \mathrm{d}\, x}_{\textbf{Exchange}} + \underbrace{\int_{\mathbb{R}^3} |H_{\text{stray}}|^2 \, \mathrm{d}\, x}_{\textbf{Stray-field}} - \underbrace{2 \int_\Omega H_{\text{ext}} \cdot m \, \mathrm{d}\, x}_{\textbf{Zeeman}}$$

Material parameter: exchange length $d = 5\text{nm}$

Variational continuum model by Landau & Lifschitz (2/2)

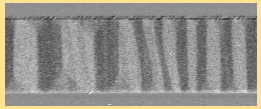

Stray field : Static Maxwell equations

$H_{\text{stray}} = -\nabla u$ satisfies

$$-\Delta u = -\nabla \cdot m \quad \text{in } \Omega \qquad \text{volume charges}$$

$$\left[\frac{\partial u}{\partial \nu}\right] = \nu \cdot m \quad \text{on } \partial\Omega \qquad \text{surface charges}$$

$$-\Delta u = 0 \quad \text{in } \mathbb{R}^3 \setminus \Omega$$

$$\int_{\mathbb{R}^3} |H_{\text{stray}}|^2 \, \mathrm{d}\, x = \int_{\mathbb{R}^3} |\nabla u|^2 \, \mathrm{d}\, x$$

A: Linear stability analysis of uniform magnetization

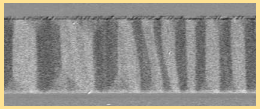

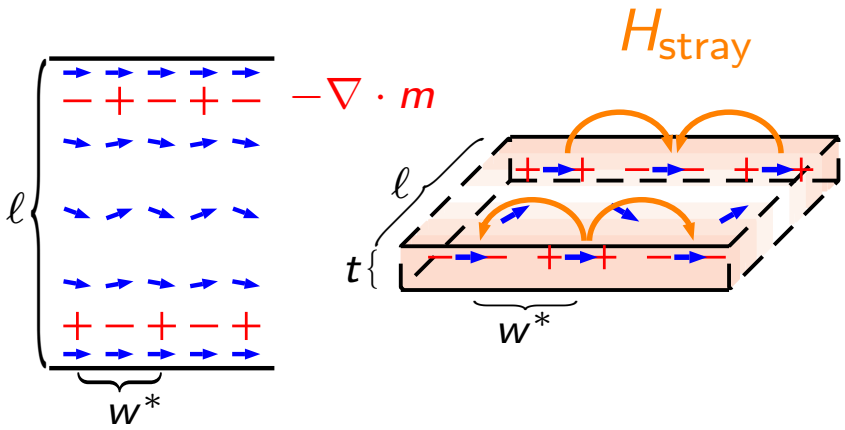

Theorem ([CAO'06])
Oscillatory buckling instability in thin wide samples $\left(\frac{d}{\ell} \ll \frac{t}{d} \ll (\frac{\ell}{d})^{1/2}\right)$

Explanation

- Exchange and stray-field energy enforce

$$m = m'(x') = (m_1, m_2)(x_1, x_2) \quad \text{in-plane}$$
$$m' \cdot \nu' = 0 \quad \text{edge-pinned}$$

- Oscillatory charges induce small stray-field energy

$$w^* \approx (32\pi d^2 \ell^2 t^{-1})^{1/3} \quad \text{optimal period}$$

A: Linear stability analysis of uniform magnetization

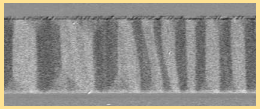

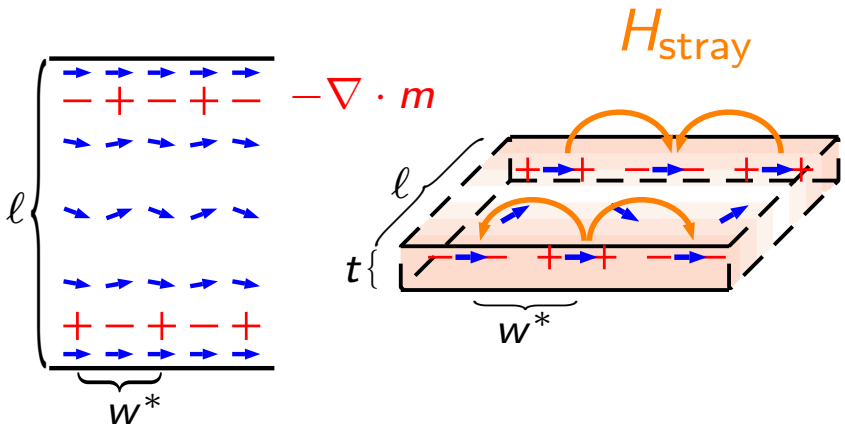

Theorem ([CAO'06])
Oscillatory buckling instability in thin wide samples $\left(\frac{d}{\ell} \ll \frac{t}{d} \ll (\frac{\ell}{d})^{1/2}\right)$

Explanation

- Exchange and stray-field energy enforce

$$m = m'(x') = (m_1, m_2)(x_1, x_2) \quad \text{in-plane}$$
$$m' \cdot \nu' = 0 \quad \text{edge-pinned}$$

- Oscillatory charges induce small stray-field energy

$$w^* \approx (32\pi d^2 \ell^2 t^{-1})^{1/3} \quad \text{optimal period}$$

Comparison with experiments

- $w_{\text{exp}} \sim w^*$ but w_{exp} is always larger than w^*

Derivation of reduced model

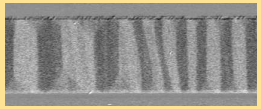

Theorem ([CAOS07]) Γ-convergence

$$E_0(m_2) = \underbrace{\int_{\Omega'} (\partial_1 m_2)^2 \,\mathrm{d}\, x'}_{\textbf{Exchange}} + \underbrace{\int_{\Omega' \times \mathbb{R}} (\partial_1 u)^2 + (\partial_3 u)^2 \,\mathrm{d}\, x}_{\textbf{Stray-field}} - \underbrace{h_{\text{ext}} \int_{\Omega'} m_2^2 \,\mathrm{d}\, x'}_{\textbf{Zeeman}}$$

Reduced Maxwell eq.

$$\begin{aligned} [\partial_3 u] &= -\partial_1 \tfrac{m_2^2}{2} + \partial_2 m_2 \quad & x_3 = 0 \\ -(\partial_1^2 + \partial_3^2) u &= 0 \quad & x_3 \neq 0 \end{aligned}$$

Ingredients

Thin film ($t \ll w^*$) implies

- $m = m'(x')$ and $m' \cdot \nu' = 0$
- Volume charges act as surface charges

- Wide film ($w^* \ll \ell$) implies $\partial_2 m'$ and $\partial_2 u$ negligible
- Small angles $m \approx m^*$ imply $m_1 = \sqrt{1 - m_2^2} \approx 1 - \frac{m_2^2}{2}$

Numerical simulation of reduced energy E_0

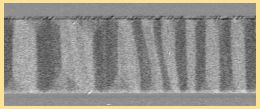

Discretization of $E_0(m_2)$

- Finite-difference scheme
- FFT for stray-field energy
- Parallelization and implementation in PETSc

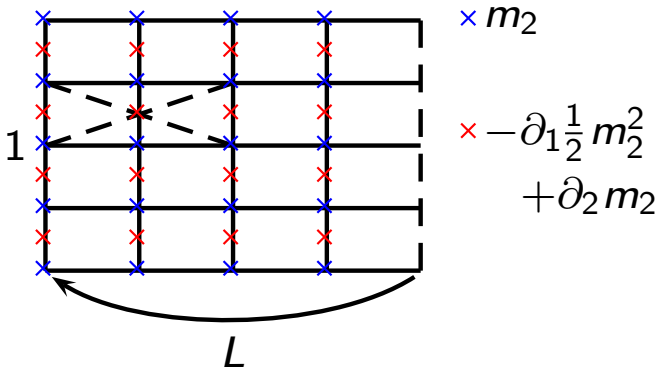

Finite-difference scheme

Numerical simulation of reduced energy E_0

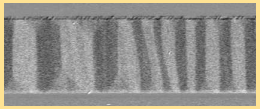

Discretization of $E_0(m_2)$

- Finite-difference scheme
- FFT for stray-field energy
- Parallelization and implementation in PETSc

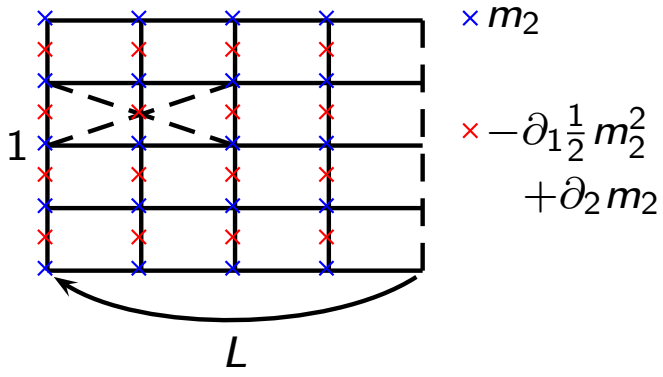

Finite-difference scheme

Computation of stationary points

- Newton's method or steepest descent
- Path following for Euler-Lagrange eq.

$$\begin{pmatrix} \nabla_{m_2} E_0(m_2^i, h_{\text{ext}}^i) \\ ((m_2^i, h_{\text{ext}}^i) - p^i) \cdot t^{i-1} \end{pmatrix} = 0$$

- Bifurcation detection and branch switching

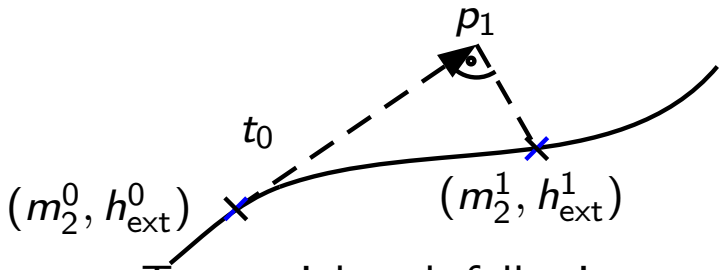

Tangential path-following

A/B: Numerical path following

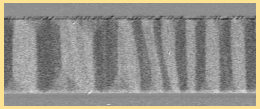

Sections of the energy landscape close to critical field h^*_{ext}

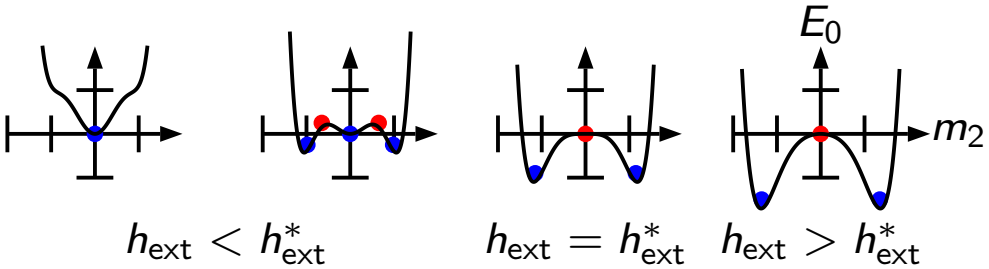

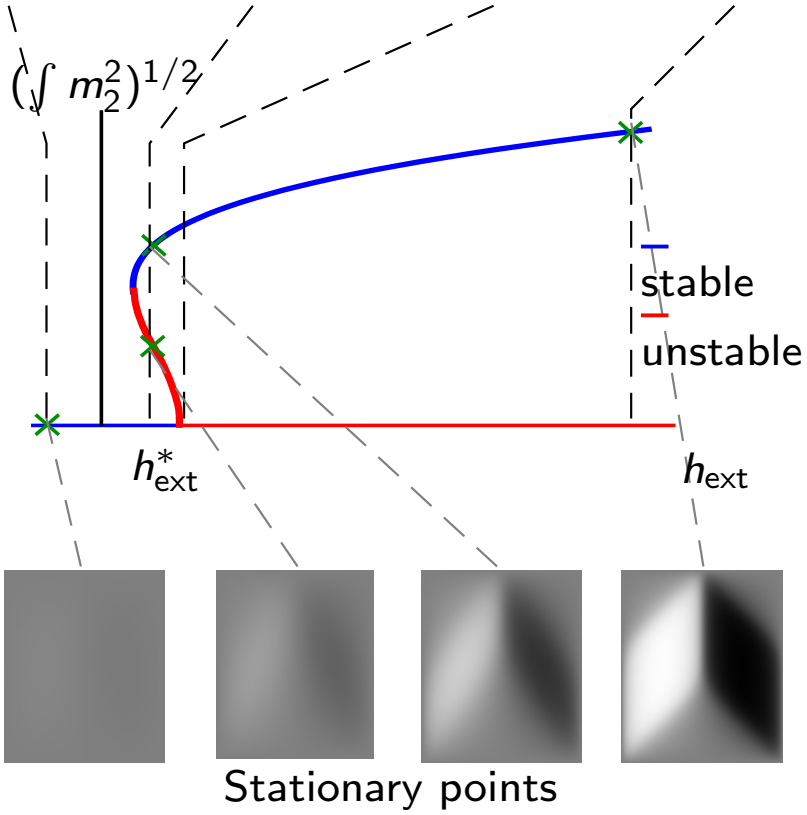

Observations

- Sub-critical bifurcation and turning point
- Mesoscopically charge-free domain-wall pattern
  $-\partial_1 \frac{m_2^2}{2} + \partial_2 m_2 = 0$
  $\Leftrightarrow$
  Shocks of Burgers eq.

C: Numerical bifurcation detection

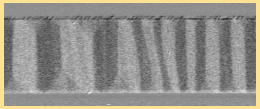

Stability of w^*-periodic branch under Nw^*-periodic perturbations?

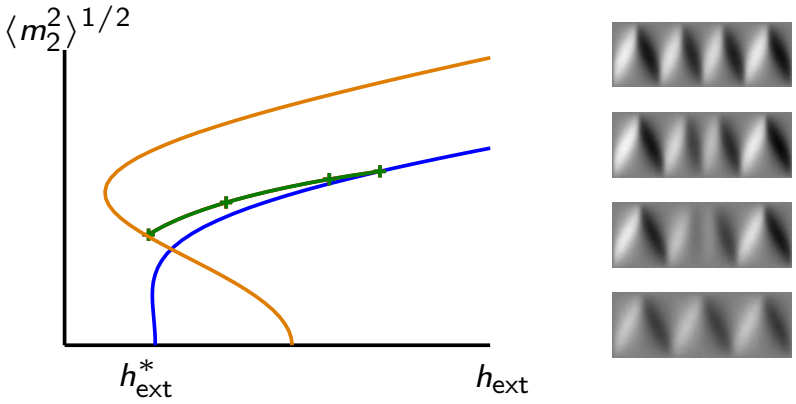

Secondary, w- and $\frac{4}{3}w$-periodic branch

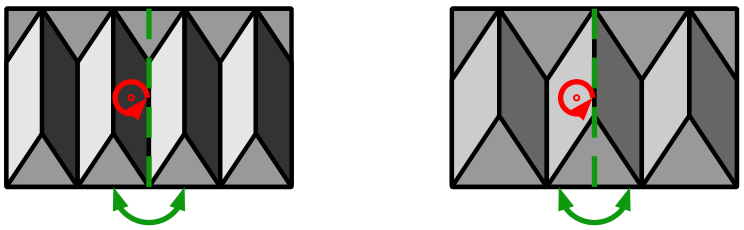

Rotation and reflection symmetry

Observations

- Cascade of instabilities
- Coarsening along secondary branches
- Degenerate bifurcations due to symmetries

C: Sharp-interface model for $h_{\text{ext}} \gg 1$

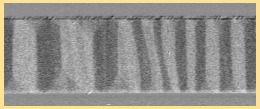

Piecewise constant **Ansatz**

- period w
- transverse component $m_2 = \pm A$
- weak divergence-free $[(-\frac{m_2^2}{2}, m_2) \cdot \nu] = 0$

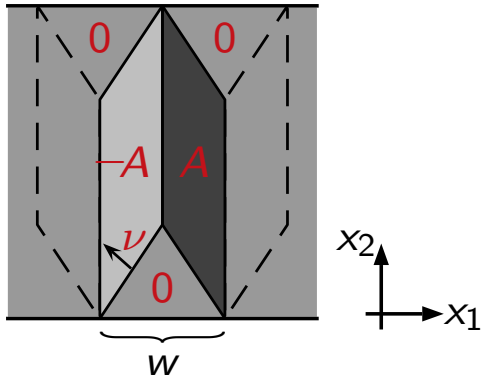

Energy

$$E_\sharp(A, w, h_{\text{ext}}) = \int_{\text{jump set}} e([m_2])\, \mathrm{d}\,\mathcal{H}^0\, \mathrm{d}\, x_2 - h_{\text{ext}} \int_{\Omega'} m_2^2\, \mathrm{d}\, x'$$

Line energy $e([m_2]) = \frac{\pi}{8} A^4 \ln^{-1}(A^2 w)$, jump $[m_2] = 2A$

C: Sharp-interface model for $h_{\text{ext}} \gg 1$

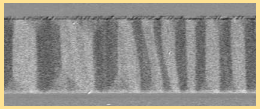

Piecewise constant **Ansatz**

- period w
- transverse component $m_2 = \pm A$
- weak divergence-free $[(-\frac{m_2^2}{2}, m_2) \cdot \nu] = 0$

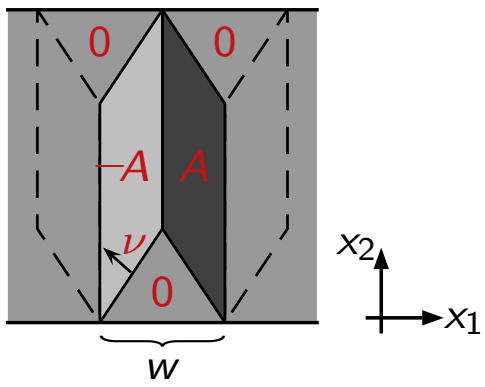

Energy

$$E_\sharp(A, w, h_{\text{ext}}) = \int_{\text{jump set}} e([m_2])\, \mathrm{d}\,\mathcal{H}^0\, \mathrm{d}\, x_2 - h_{\text{ext}} \int_{\Omega'} m_2^2\, \mathrm{d}\, x'$$

Line energy $e([m_2]) = \frac{\pi}{8} A^4 \ln^{-1}(A^2 w)$, jump $[m_2] = 2A$

Optimal period

Minimization of energy per length $\frac{E_\sharp}{w}$ in A and w

$$w \sim h_{\text{ext}} \ln h_{\text{ext}}$$

C: Geometric criterion for the secondary instabilities

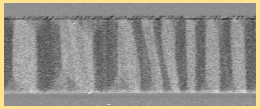

Concavity of minimal energy per period, i.e.,

$$\min_A E_\sharp(A, w),$$

in $w \Rightarrow$ modulation instability

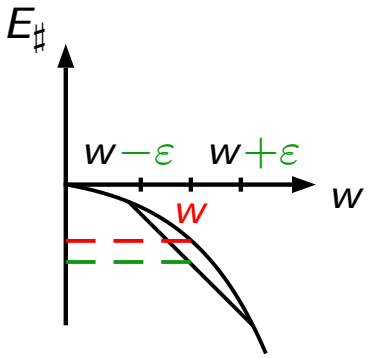

$$2E_\sharp(w) > E_\sharp(w+\epsilon) + E_\sharp(w-\epsilon)$$

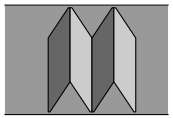

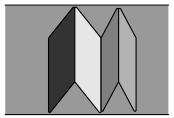

C: Geometric criterion for the secondary instabilities

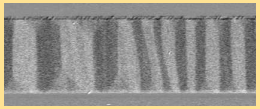

Concavity of minimal energy per period, i.e.,

$$\min_A E_\sharp(A, w),$$

in $w \Rightarrow$ modulation instability

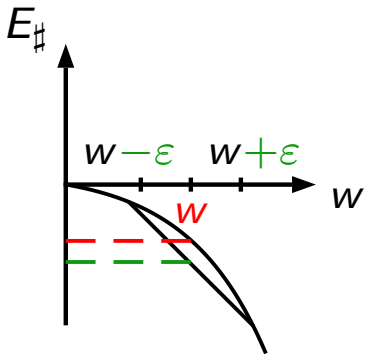

$$2E_\sharp(w) > E_\sharp(w+\epsilon) + E_\sharp(w-\epsilon)$$

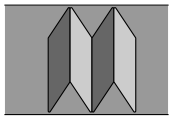

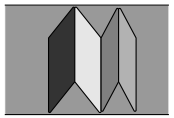

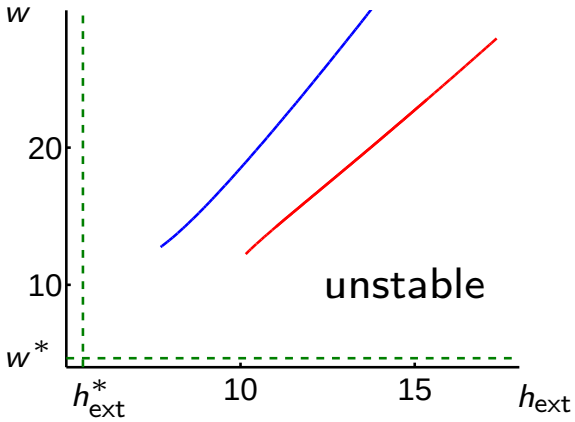

$E_\sharp$: optimal and marginally stable period

C: Geometric criterion for the secondary instabilities

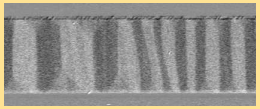

Concavity of minimal energy per period, i.e.,

$$\min_A E_\sharp(A, w),$$

in $w \Rightarrow$ modulation instability

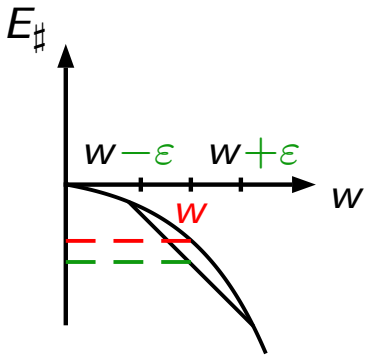

$$2E_\sharp(w) > E_\sharp(w+\epsilon) + E_\sharp(w-\epsilon)$$

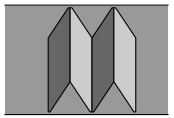

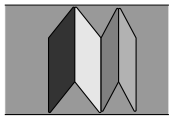

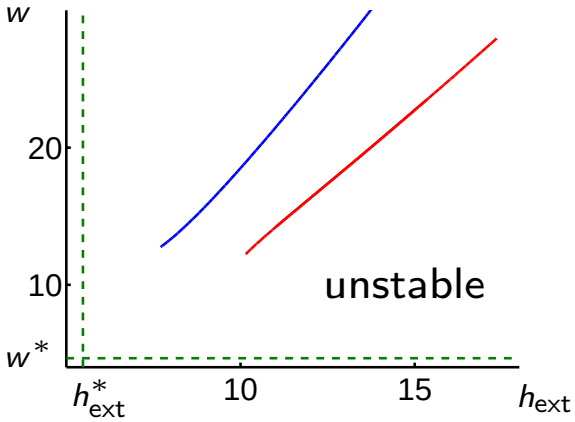

$E_\sharp$: optimal and marginally stable period

Caution!

- Sharp-interface model is rigid
- Reduced energy is non-local

$E_0\Big($  $\Big) \stackrel{?}{=} E_0\Big($ 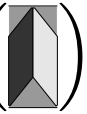 $\Big) + E_0\Big($ 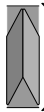 $\Big)$

C: Instability criterion in the reduced model

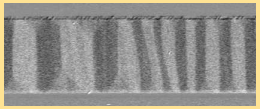

Theorem

For infinitesimal Bloch-perturbations, i.e.,

$$\delta m_2 = e^{i\epsilon x_1} g(x_1, x_2) + c.c.$$

with w-periodic g,

it holds

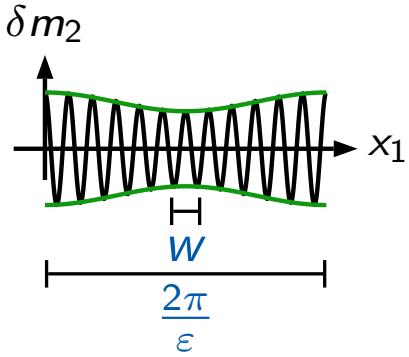

$$\lambda^{\epsilon}_{min} \leq \inf_{\delta m_2} \frac{\text{Hess } E_0(m_2)(\delta m_2, \delta m_2)}{\int\int \delta m_2^2 \,\mathrm{d}\, x_1 \,\mathrm{d}\, x_2} \lessapprox \epsilon^2 \frac{w^2 \frac{d^2}{dw^2} E_0(w)}{\int (\partial_1 m_2)^2 \,\mathrm{d}\, x_1 \,\mathrm{d}\, x_2}$$

C: Instability criterion in the reduced model

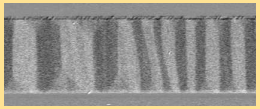

Theorem

For infinitesimal Bloch-perturbations, i.e.,

$$\delta m_2 = e^{i\epsilon x_1} g(x_1, x_2) + c.c.$$

with w-periodic g,

it holds

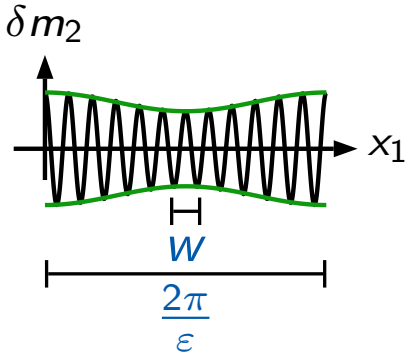

$$\lambda^{\epsilon}_{min} \leq \inf_{\delta m_2} \frac{\text{Hess } E_0(m_2)(\delta m_2, \delta m_2)}{\int\int \delta m_2^2 \, \mathrm{d}\, x_1 \, \mathrm{d}\, x_2} \approx \epsilon^2 \frac{w^2 \frac{d^2}{dw^2} E_0(w)}{\int (\partial_1 m_2)^2 \, \mathrm{d}\, x_1 \, \mathrm{d}\, x_2}$$

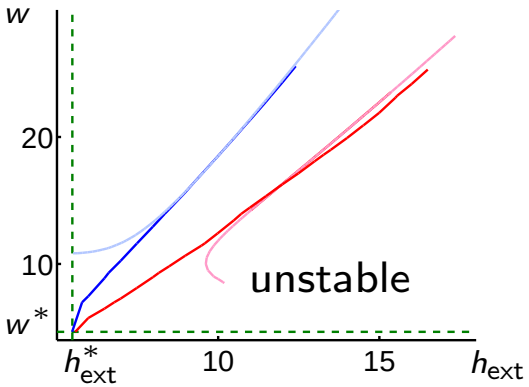

$E_\sharp$ vs. simulation of E_0

optimal and marginally stable period

C: Scaling laws for minimizers of the reduced model

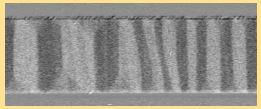

Theorem ([OS10])

Let $h_{ext} \gg 1$ *and* $L \gg h_{ext} \ln h_{ext}$.

a) Optimal period (lower bound) for almost optimal m_2*, i.e.,*

$$L^{-1} \int_0^L \int_0^1 (m_2(x_1 + w, x_2) - m_2(x_1, x_2))^2 \, \mathrm{d}\, x_2 \, \mathrm{d}\, x_1$$
$$\lesssim \left(\frac{w}{h_{ext} \ln h_{ext}} \right)^{\alpha} L^{-1} \int_0^L \int_0^1 m_2^2 \, \mathrm{d}\, x_2 \, \mathrm{d}\, x_1$$

for all $w > 0$ *and* $\alpha \in [0, \frac{2}{5})$

b) Minimal energy per length

$$\min_{m_2} L^{-1} E_0 \sim -h_{ext}^3 \ln^2 h_{ext}$$

C: Domain theory as a limit of the reduced model

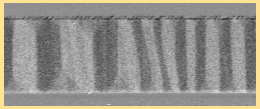

Theorem ([OS10])

Let $h_{ext} \gg 1$ and $L \sim h_{ext} \ln h_{ext}$. Let m_2 be almost optimal, i.e., $L^{-1} E_0(m_2) \sim \min_{m_2} L^{-1} E_0$. Then there exists m_2^* with

$$L^{-1} \int_0^L \int_0^1 (m_2 - m_2^*)^2 \, \mathrm{d}\, x_2 \, \mathrm{d}\, x_1 \ll L^{-1} \int_0^L \int_0^1 (m_2)^2 \, \mathrm{d}\, x_2 \, \mathrm{d}\, x_1$$

such that

$$-\partial_1 \frac{(m_2^*)^2}{2} + \partial_2 m_2^* = 0$$

distributionally.

A: Deviation of w^* and w_{exp} and stability close to h^*_{ext}

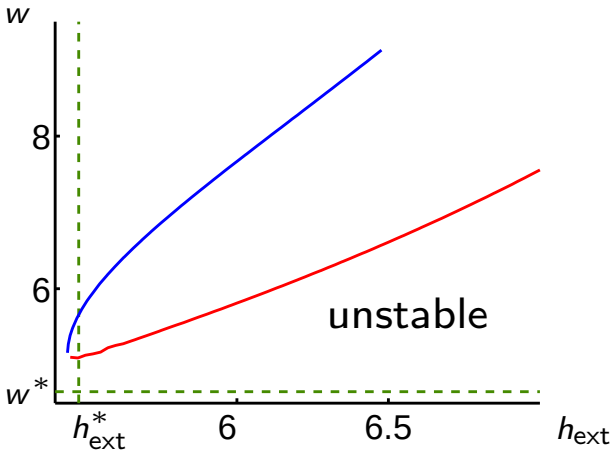

optimal and marginally stable

period close to h^*_{ext}

Numerical simulation of reduced energy

- Pattern of period w^* is unstable
- Minimal stable period

A: Extended bifurcation analysis of E_0 close to h^*_{ext}

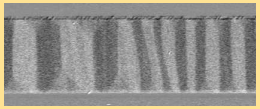

- Perturbations of critical field and critical wave number

$$h_{\text{ext}} \;=\; h^*_{\text{ext}} + \delta h_{\text{ext}} \quad \text{and} \quad k \;=\; \frac{2\pi}{w} \;=\; k^* + \delta k$$

- Perturbations of unstable mode

$$m_2 \;\approx\; A\, m_2^* + A^2\, m_2^{**} + A^3\, m_2^{***}$$

yield asymptotic expansion of the reduced energy

$$E_0(A, \delta k, \delta h_{\text{ext}}) \;\approx\; (-c_2\, \delta h_{\text{ext}} + \tilde{c}_2\, \delta k^2)\, A^2 + (-c_4 + \tilde{c}_4\, \delta k)\, A^4 + c_6\, A^6$$

- $|c_4| \ll 1 \Leftrightarrow$ Asymmetric side-band instability
- Eckhaus instability in convective systems

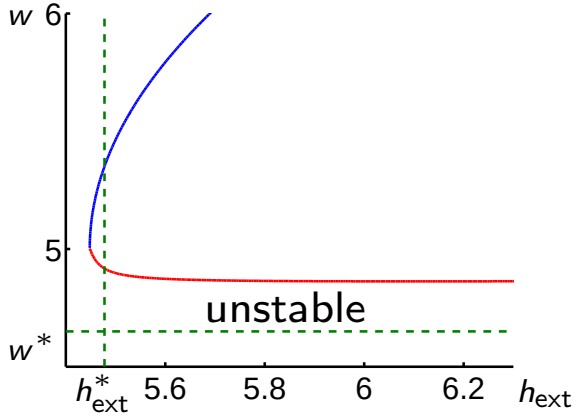

optimal and marginally stable period

Polycrystalline anisotropy (1/2)

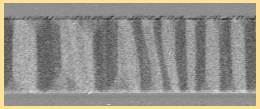

. . . causes ripple and perturbed concertina in the experiments

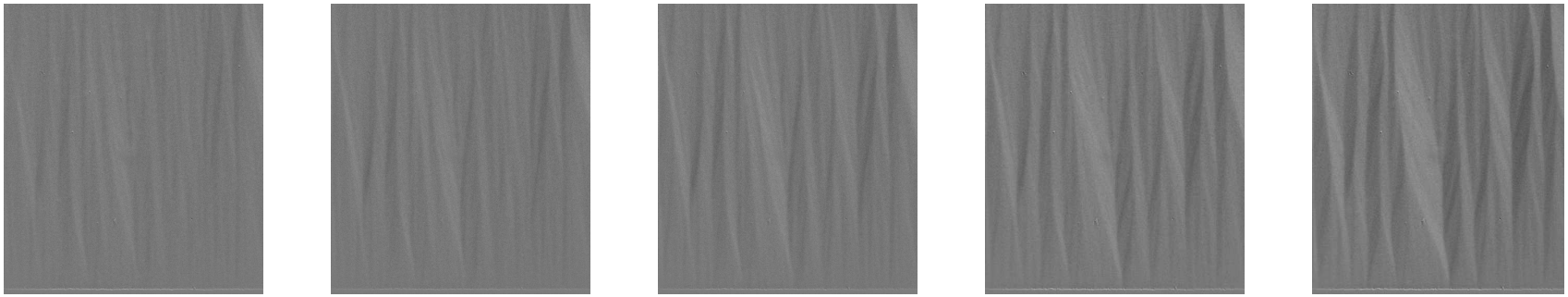

Permalloy $t = 30\text{nm}$, $\ell = 70\mu\text{m}$

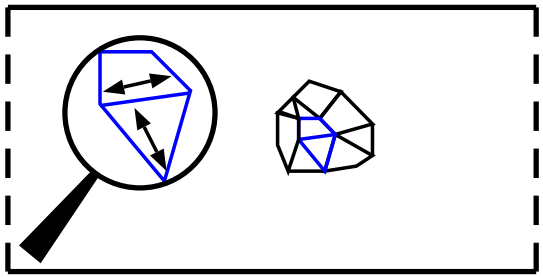

position-dependent easy axis $e(x_1, x_2)$ of strength Q

$$-Q \int_\Omega (m \cdot e(x_1, x_2))^2 \, \mathrm{d}\, x$$

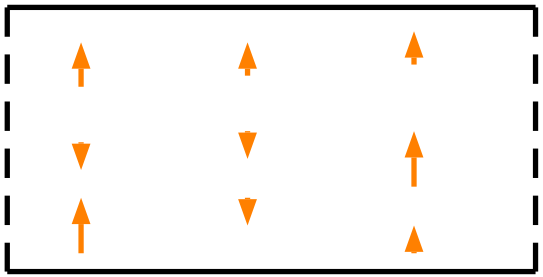

transverse stochastic field $h^{\text{ripple}} = Q e_1 e_2$

$$-2t \int_{\Omega'} h^{\text{ripple}} m_2 \, \mathrm{d}\, x'$$

Polycrystalline anisotropy (2/2)

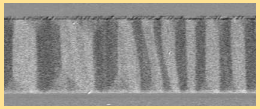

Ripple and concertina in experiment (o.) and simulation (u.)

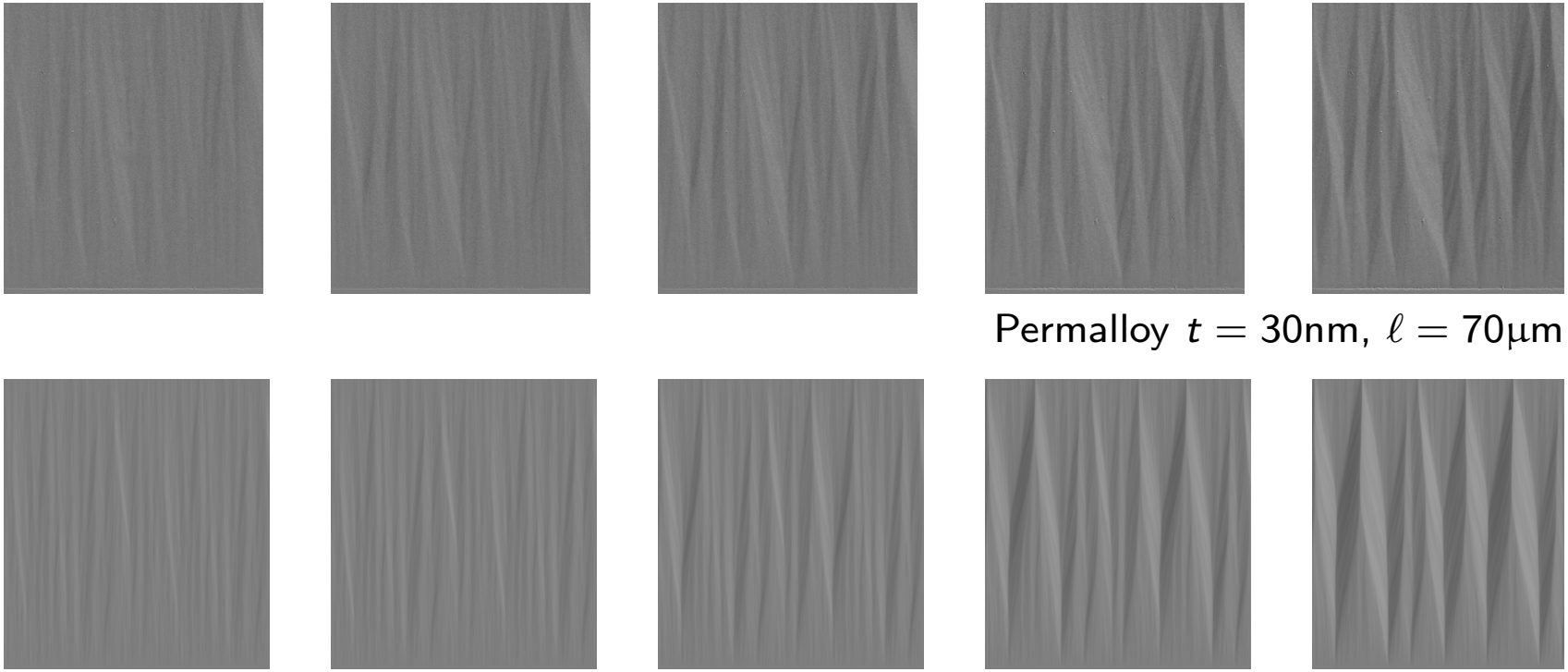

Permalloy $t = 30\text{nm}$, $\ell = 70\mu\text{m}$

Linearization of the energy

Confirmation of smooth transition of ripple to concertina

$$\lim_{h_{\text{ext}} \uparrow h^*_{\text{ext}}} \langle | {k_1}^{\text{ripple}} | \rangle = k_1^*$$

Summary

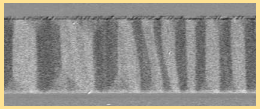

- Understanding of observations by exploration of the energy landscape

  Simulation (path following, ...)

  $\Leftrightarrow$

  Asymptotic analysis

  (bifurcation analysis, Bloch-waves, ...)

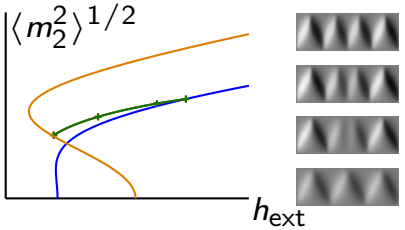

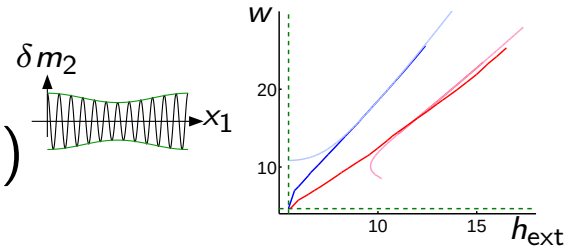

- Extension of reduced model (polycrystalline anisotropy)

Further aspects

- Anisotropy and large angles
- Finite sample size
- Refining and hysteresis
- Amplitude functional

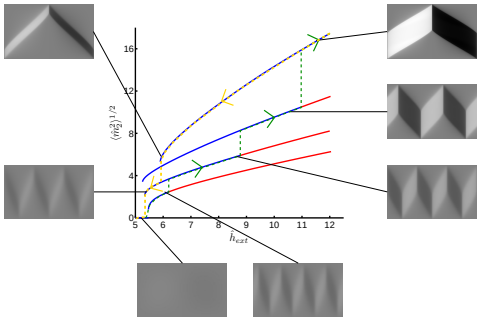

Finite sample size: Van den Berg's explanation

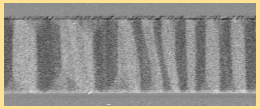

	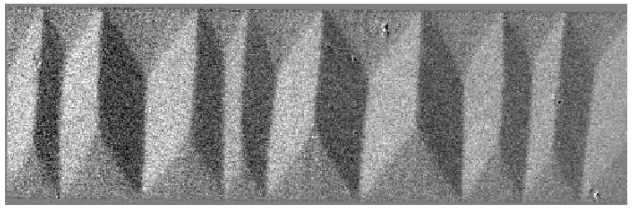	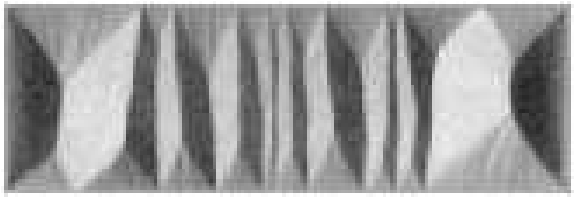
Geometry	Length $L \gg \ell$	Length $L \sim \ell$
External field	Critical field $h^*_{\text{ext}} \approx 3(\frac{\pi}{2})^{4/3}(d^2\ell^{-4}t^2)^{1/3} - Q$	$h^{\text{begin}}_{\text{ext}} \sim \frac{t}{\ell}$ $h^{\text{end}}_{\text{ext}} \sim t\ell L^{-2} \ln t\ell^{-1}$
length scale	$w^* \sim d^{2/3}\ell^{2/3}t^{-1/3}$	$w \sim \ell$
Formation	Simultaneously along sample	Successive in-growth from tips

Example: Permalloy of transverse anisotropy $Q = 5.0 \times 10^{-4}$ and dimension $\ell = 30\mu\text{m}$, $t = 30\text{nm}$

$$h^{\text{begin}}_{\text{ext}} \sim 1 \times 10^{-3} \gg h^*_{\text{ext}} \approx 3.4 \times 10^{-4} \gg h^{\text{end}}_{\text{ext}} \sim 1.6 \times 10^{-6}$$

Experiment vs. Analysis: The period of the instability

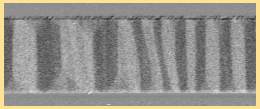

Measurements for Permalloy samples of length $\ell = 10 \ldots 50\mu\text{m}$ and thickness $t = 10 \ldots 150\text{nm}$

Range of theoretical period $\frac{w^*}{w^*(\ell_{\text{min}}, t_{\text{max}})}$

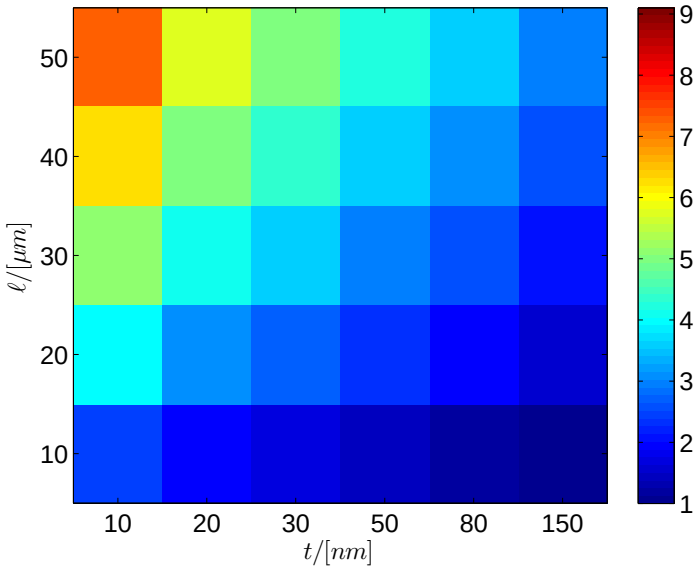

Comparison of experimental and theoretical period $\frac{w_{\text{exp}}}{w^*}$

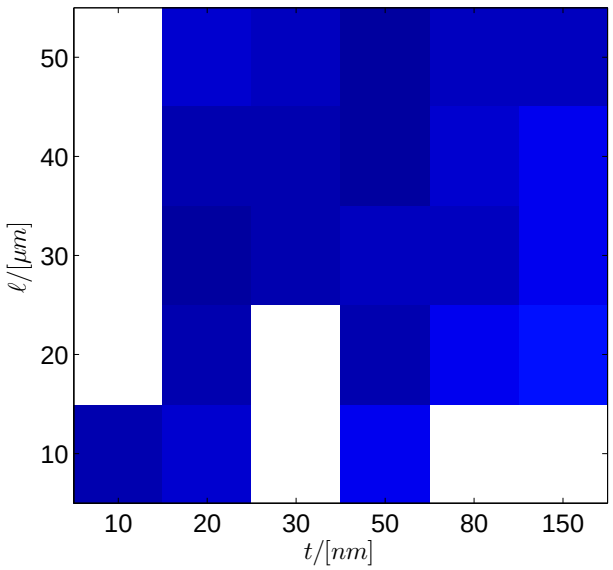

Simulation – Hysteresis loop